Sensor Position Estimation Method for IoT Using Mobile Reference Node

JACEK STEFANSKI[iD], **(Member, IEEE), AND JAROSLAW SADOWSKI**

Faculty of Electronics, Telecommunications, and Informatics, Gdansk University of Technology, 80-233 Gdansk, Poland

Corresponding author: Jacek Stefanski (jstef@eti.pg.edu.pl)

ABSTRACT The paper proposes an innovative method of locating objects for the Internet of Things (IoT). The proposed method allows the position of a fixed measuring sensor (MS) to be estimated using one mobile base station with a known position moving around the MS. The mathematical analysis of the method, and three algorithms — Newton's (NA), gradient descent (GD) and genetic (GA) — for solving the system of non-linear positional equations are presented. Next, the analysis of the position dilution of precision (PDoP) parameter for the proposed method, and the Cramér-Rao lower bound (CRLB), limiting the accuracy of the method, are presented. Finally, the results of complex simulation studies on the efficiency of the proposed method for various selected system parameters of the sensor network and convergence of the algorithms used to solve the system of non-linear equations are described.

INDEX TERMS Asynchronous transfer mode, radio navigation, wireless sensor networks, IoT.

I. INTRODUCTION

The Internet of Things (IoT) is a concept according to which uniquely identifiable things or objects can directly or indirectly collect, process and/or exchange data via telecommunication (radio communication) networks. These types of items include, but are not limited to, household, garden and agricultural appliances, lighting and heating units, as well as consumable appliances worn by people or animals [12]. The IoT offers great potential to change the way in which systems function, often without the need for human interaction or involvement. The ability to efficiently collect data starts with the use of sensors. Sensors are devices that respond to inputs from the physical world and then take those inputs and display them, transmit them for additional processing, and/or use them in conjunction to make decisions and/or adjust operating conditions. Common IoT sensors that may be employed include: temperature sensors, pressure sensors, motion sensors, level sensors, image sensors, proximity sensors, water quality sensors, chemical sensors, gas sensors, smoke sensors, infrared sensors, acceleration sensors, gyroscopic sensors, humidity sensors, and optical sensors [27].

An indispensable element of a properly functioning IoT are all kinds of telecommunication networks through which information is exchanged between the things or objects
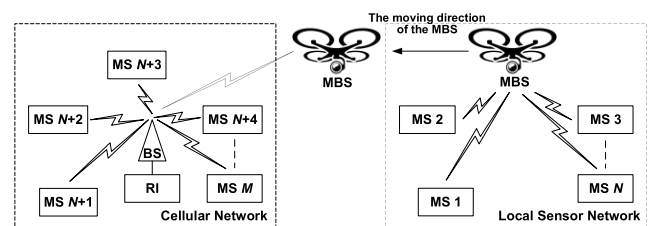
FIGURE 1. An example of how to integrate the local sensor network with a cellular network.

defined above. A problem in the functioning of the IoT appears when the objects assigned to the IoT are outside of the operating area of telecommunication networks. One of the methods of transmitting information for the IoT, especially when collected outside of the area of cellular networks, is shown in Fig. 1 [16].

Measuring sensors (MSs) within the local sensor network (LSN) continuously collect information that is periodically transmitted in the direction of a mobile reference node, called a mobile base station (MBS), which is regularly moving around the area of network operation and may be mounted, e.g. on a drone. Apart from a navigation module (e.g. a GPS signal receiver), the MBS is equipped with a module for data collection and further transmission. For the MBS, the direction of movement between the MSs in the LSN area and the base station (BS), which belongs to the cellular

network (CN), is determined. After collecting information from individual MSs within the LSN, the MBS navigates with the help of the navigation module to the area of the cellular network, and then, after connecting to the BS, transmits the collected information to the recipient of information (RI). The use of the proposed concept significant increases the range of telecommunication networks for the IoT.

Many localization algorithms and systems have been developed for both indoor and outdoor environments. Location service (LCS) is a primary service of the IoT, while localization accuracy is a key issue. To achieve higher localization accuracy, extra hardware equipment is utilized [7]. Many researchers have significant interest in the IoT, and have implemented many creative advancements for LCS. As we know, there are several techniques available for location service such as angle of arrival (AoA), received signal strength (RSS), time of arrival (ToA), time difference of arrival (TDoA), and a combination of these [3], [13], [17], [18], [22], [23].

All of the described methods need appropriate network infrastructure in the form of base (reference) stations, synchronization mechanisms in the sensor network, and many other necessary elements for proper operation. The localization method proposed in this paper minimizes the network infrastructure and belongs to asynchronous methods [19], [20], [24], [25].

There are many potential applications for the proposed method, such as:

- the temporary location of farm animals in an area of difficult-to-reach pastures,
- the temporary location of animals living in the wild in areas outside of the range of telecommunications infrastructure,
- periodically checking the position of soldiers in an unknown area,
- periodically checking the position of free-floating measuring buoys on water bodies, and many more.

This paper is organized as follows: Section II describes the proposed method. In Section III, a mathematical analysis of the method is presented, and three algorithms — Newton's (NA), gradient descent (GD) and genetic (GA) — dedicated to solving the system of non-linear positional equations for the method, are described. The next two sections present the position dilution of precision, and the Cramér-Rao lower bound (CRLB) for the proposed method, respectively. Section VI is divided into four subsections, which present the simulation model used for the study, an analysis of the position dilution of precision (PDoP) parameter for the proposed variants of the sensor network configuration, as well as the obtained CRLB values, and the efficiency of the proposed locating method. Finally, the last section concludes the paper.

II. DESCRIPTION OF THE PROPOSED METHOD

The architecture of radiolocation sensor networks is usually based on a set of fixed base stations (BS) and a measuring

sensor (MS) equipped with appropriate technical means, whose location is sought [6], [14]. In sensor networks, the position of a measuring sensor is often estimated on the basis of the radio signals emitted by the MS. In this case, the sensor network is responsible for the implementation of appropriate measurements of radio signal parameters and for MS position estimation. In the problem under consideration, it is assumed that the MS transmits its measurement data in one direction. These signals are then received by a mobile base station (MBS), e.g. a drone, which on the basis of the measured time dependencies and knowledge of its own position, estimates the position of the MS. Then, the proposed method uses the knowledge of virtual differences in propagation times of radio signals between the MBS with a known position and the MS, whose position is wanted.

The proposed new method is passive and based on the reception of signals transmitted by a localized MS, where the repetition time of these signals may or may not be known. In general, the structure of a radio sensor network in which this method can be implemented is shown in Fig. 2.
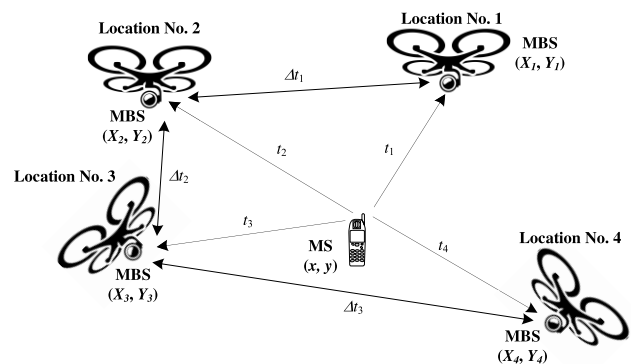
FIGURE 2. An example of a sensor network structure in which the proposed method can be implemented.

The measuring sensor transmits location signals with a known or unknown (but constant) repetition rate. In the case under consideration, the mobile base station works asynchronously to the MS — it takes measurements in the rhythm of its own internal clock. The MBS, moving around the MS (from Location No. 1 to Location No. 4), measures virtual differences in the propagation time of the radio signals transmitted from MS Δt_i, where $i = 1, 2$ and 3 (for the 2D case). The radio signals from the MS are measured by the MBS at known locations (X_i, Y_i) at the i-th point (for example, from the GPS system — the drone's position indicated by the GPS receiver is usually given in three dimensions; to simplify further analysis, the drone's position has been projected onto a plane, hence only two coordinates), (x, y) are the MS coordinates, and t_i represent time delays of radio signal propagation between the MS and the MBS. The MBS does not need to stop at a known location in order to carry out the relevant measurements. This is due to the assumption that the speed of the propagation of the electromagnetic wave is much greater than the speed of the MBS. The resulting measurement errors

are therefore negligible. It is more important to determine the exact position of the MBS during the measurements, which is examined later in the paper. Thanks to the numbering of the location signals transmitted by the MS, the MBS is able to estimate the position of the measuring sensor. The time sequences illustrating the principle of operation of the proposed method are shown in Fig. 3.
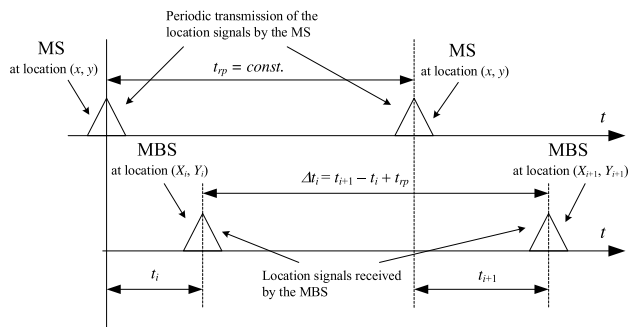

FIGURE 3. Time flows illustrating the principle of operation of the proposed method.

At the top of this diagram, two consecutive points in time are marked in which the MS sends location signals with the repetition period t_{rp}. The period t_{rp} must be constant even if not known by the MBS. During this time, the MBS changes its position and receives location signals at two known locations (X_i, Y_i) and (X_{i+1}, Y_{i+1}). The MBS position change is key in the MS position estimation process. The MBS measurements in different positions enables the necessary parameters of the received signals to be determined in the process of locating the MS. The process of position estimation is carried out in the MBS. Based on the knowledge of the mobile base station coordinates, radio wave propagation velocity, and virtual differences in radio signal propagation times Δt_i (for $i = 1, 2, 3$), it is possible to estimate the coordinates of the MS.

In the proposed method, it is important to accurately measure the arrival time of the radio signal from the MS. Thus, the signal processing time in the MBS is not important, as long as it does not affect the results obtained (e.g. the same processing time for all received signals). This method requires a minimum of four radio signals to be collected from the MS during the movement of the MBS around the MS. On receiving the fourth signal, the MBS can estimate the MS's location. Thus, it can be concluded that the described method is a real-time method.

The next section will present a detailed mathematical analysis of the proposed radiolocation method.

III. CALCULATING THE POSITION OF THE OBJECT

Let's assume that we have N positioning signals received by the MBS at points with known coordinates. For a two-dimensional case, the individual MBS coordinates can be written as (X_i, Y_i). The MS transmits location signals with the t_{rp} repetition period, which is constant and unknown. The MBS measures virtual distance differences Δd_i between

observation points in time $(i = 1, \ldots, N\text{-}1)$

$$\Delta d_i = v \cdot (t_{i+1} - t_i) + v \cdot t_{rp} = d_{i+1} - d_i + d_{rp}$$
$$= \sqrt{(X_{i+1} - x)^2 + (Y_{i+1} - y)^2}$$
$$- \sqrt{(X_i - x)^2 + (Y_i - y)^2} + d_{rp} \quad (1)$$

where v represents the propagation speed of radio signals in the propagation medium (it can be approximately assumed that v is equal to the speed of light in a vacuum, $c \approx 3 \cdot 10^8$ m/s), t_{i+1} and t_i describe the propagation times of the localization signals from the MS to the i-th position of the MBS, and (x, y) are the MS coordinates. At this point, it is worth noting that Δd_i are hypothetical distance differences, which result from real distance differences between the localized MS and the MBS in various known locations, and the distance travelled by the radio waves in the time interval determined by the period of repeating localization signals ($d_{rp} = v \cdot t_{rp}$).

The above relationship can be used to estimate the position of the measuring sensor (x, y) assuming that the following are known:

- coordinates of the mobile base station,
- virtual differences in distance Δd_i between the MBS and the MS.

In the literature on the subject, it is difficult to find direct algorithms that lead to the solution of systems of non-linear equations described by relationship (1). For the purposes of this study, three well-known algorithms have been adapted to solve the problem raised in this paper:

- Newton's algorithm (NA) – a generalized approach that Foy used in his algorithm [8],
- gradient descent algorithm (GD) [7],
- genetic algorithm (GA) [10].

Assuming the simplest two-dimensional case and $N = 4$, the problem of MS position estimation in the presented method boils down to solving a system of non-linear equations of the forms

$$\begin{cases} \Delta d_1 = \sqrt{(X_2 - x)^2 + (Y_2 - y)^2} \\ \qquad - \sqrt{(X_1 - x)^2 + (Y_1 - y)^2} + d_{rp} \\ \Delta d_2 = \sqrt{(X_3 - x)^2 + (Y_3 - y)^2} \\ \qquad - \sqrt{(X_2 - x)^2 + (Y_2 - y)^2} + d_{rp} \\ \Delta d_3 = \sqrt{(X_4 - x)^2 + (Y_4 - y)^2} \\ \qquad - \sqrt{(X_3 - x)^2 + (Y_3 - y)^2} + d_{rp} \end{cases} \quad (2)$$

By determining the d_{rp} from the above first equation and inserting it into the two others, we obtain

$$\mathbf{f}(x, y) = \begin{cases} \Delta d_2 - d_3 + 2 \cdot d_2 - d_1 - \Delta d_1 \\ \Delta d_3 - d_4 + d_3 + d_2 - d_1 - \Delta d_1 \end{cases} \quad (3)$$

Therefore, as long as d_{rp} (t_{rp}) is constant, knowledge of the exact d_{rp} value is not necessary for MS position estimation.

Based on [5], the linearized version of the above system of equations can be written as

$$\mathbf{J}(x, y) \cdot \mathbf{h} = -\mathbf{f}(x, y) \qquad (4)$$

where $\mathbf{J}(x, y)$ is the Jacobian matrix described by (5), and vector $\mathbf{h} = [h_x, h_y]^T$ represents the correction of the MS coordinates in subsequent iterations,

$$\mathbf{J}(x, y) = \begin{bmatrix} \dfrac{X_1 - x}{d_1} + \dfrac{2 \cdot (x - X_2)}{d_2} + \dfrac{X_3 - x}{d_3} \\ \dfrac{X_1 - x}{d_1} + \dfrac{x - X_2}{d_2} + \dfrac{x - X_3}{d_3} + \dfrac{X_4 - x}{d_4} \\ \dfrac{Y_1 - y}{d_1} + \dfrac{2 \cdot (y - Y_2)}{d_2} + \dfrac{Y_3 - y}{d_3} \\ \dfrac{Y_1 - y}{d_1} + \dfrac{y - Y_2}{d_2} + \dfrac{y - Y_3}{d_3} + \dfrac{Y_4 - y}{d_4} \end{bmatrix} \qquad (5)$$

All algorithms used to estimate the position of the measuring sensor have been implemented in MATLAB. Appendix A presents pseudocodes of the first two algorithms, i.e. Newton and gradient descent.

The last algorithm that is applied to estimate the position of a MS in the proposed system is a genetic algorithm, in which evolutionary-probabilistic rules are used to select and create new solutions. This algorithm uses natural phenomena occurring at the cellular level, which are related to chromosomes, genes and evolutionary transitions of genetic material from generation to generation. In addition, GA enables the search for a solution at many points simultaneously, and in principle is free from the limitations imposed on the space of search (e.g. continuity and existence of derivatives of the target function). A disadvantage of GA is that the solution sought does not always seek to achieve a real global minimum. On the other hand, this algorithm is characterized by versatility in solving various problems, and simplicity of implementation. The schematic mode of operation of a genetic algorithm for solving non-linear equations is presented in Fig. 4. This scheme was used to develop the function in the MATLAB environment. At the beginning of the algorithm, it is necessary to define the conditions of its termination, i.e. the threshold value of the target function — in our case, it is a norm of vector $\mathbf{f}$ described by (3) — and the maximum number of iterations in case of failure to reach the given accuracy threshold. Next, a given number of potential solutions (w) should be randomly generated from a predefined area (initial population of chromosomes). For each solution (chromosome) the values of the target function are calculated. Next, the chromosomes are sorted according to the value of the target function (it is assumed that the lower the value of the target function, the closer the solution represented by the chromosome is to the real one). Half of the group of the least matched chromosomes is rejected, while the group of chromosomes ($1/2 \cdot w$) for which the values of the target function are closest to the assumed precision threshold is used to generate a new population of chromosomes (new potential solutions) in the process of so-called mutation and crossing
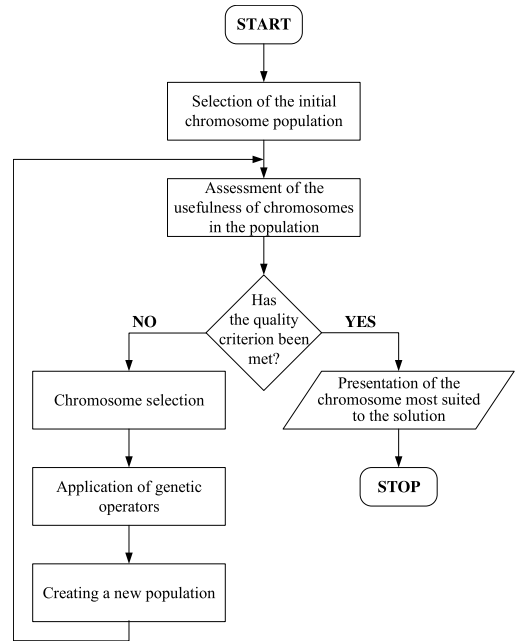

FIGURE 4. Schematic diagram of the genetic algorithm for solving non-linear equations.

of solutions — analogous to biological evolution processes (genetic operators).

The next step of the algorithm is a new process of sorting all potential solutions. The algorithm described above is repeated until a preset precision threshold is reached (the solution represented by the chromosome with the lowest value of the target function) or a preset number of iterations, when the search process does not reach the assumed accuracy.

IV. POSITION DILUTION OF PRECISION FOR THE PROPOSED METHOD

In classical radiolocation systems, based on measurements of distance or distance difference between a localized object and reference stations, the accuracy of position estimation depends to a large extent on the geometric distribution of reference stations in relation to the localized object. It is characterized by the position dilution of precision parameter, which is a measure of the influence of measurement errors on the position estimation [26]. The higher the value of this parameter, the lower the accuracy of the position estimation in the radiolocation system that can be obtained despite maintaining a constant level of accuracy of measurements of the radio signal parameters. The PDoP coefficient can be determined on the basis of the Jacobian matrix, built of partial derivatives (first order) of linearized positional equations adjusted to the given method

$$\mathbf{J} \cdot \Delta \mathbf{x} = \Delta \mathbf{d} \qquad (6)$$

where $\mathbf{J}$ represents the Jacobian matrix, while $\Delta \mathbf{x}$ is a vector containing, among others, the coordinates of the localized object, and $\Delta \mathbf{d}$ is a vector consisting of the measured distances or distance differences between reference stations and

the localized object, depending on the method. With such a defined problem, the PDoP coefficient can be determined from the relation [1, 21]

$$P_D = \sqrt{tr[(\mathbf{J}^T\mathbf{J})^{-1}]} \tag{7}$$

where $tr[\cdot]$ is the trace of the matrix. The lower the value of the PDoP, the more advantageous the positioning of the reference stations because it translates into a smaller position error. A PDoP value below unity indicates a redundant configuration of reference stations. A value of the PDoP coefficient above 20 translates into a significant location error due to the mismatched distance between the reference stations and the object.

V. CRAMÉR-RAO LOWER BOUND

An extremely important parameter describing the potential effectiveness of the radiolocation system is the Cramér-Rao lower bound, which defines the minimum mean square error of an unbiased estimator, which is a solution of a system of equations describing the applied localization method [15]. For an unbiased case, and assuming that $\boldsymbol{\theta}$ is an unknown deterministic vector, which is estimated using the $\boldsymbol{\rho}$ observation vector from the probability distribution of the density $p(\boldsymbol{\rho};\boldsymbol{\theta})$, the variance of any unbiased $\hat{\boldsymbol{\theta}}$ – estimator of vector $\boldsymbol{\theta}$ – is limited from the bottom by the inverse of the so-called Fisher information matrix [11]

$$\mathrm{var}\left(\hat{\boldsymbol{\theta}}\right) \geq \frac{1}{\mathbf{I}(\boldsymbol{\theta})} \tag{8}$$

where

$$\mathbf{I}(\boldsymbol{\theta}) = -E\left[\frac{\partial^2 \ln p(\boldsymbol{\rho};\boldsymbol{\theta})}{\partial \boldsymbol{\theta}^2}\right] \tag{9}$$

and $E[\bullet]$ is the expected value. In radiolocation systems for Gaussian error distribution of measurements, $p(\boldsymbol{\rho};\boldsymbol{\theta})$ takes the following form

$$p(\boldsymbol{\rho};\boldsymbol{\theta}) = -\frac{1}{\sqrt{2\pi\sigma^2}}\exp\left[-\frac{1}{2\sigma^2}(\boldsymbol{\rho}-\boldsymbol{\theta})^2\right] \tag{10}$$

The starting point for deriving the Cramér-Rao lower bound for the proposed method is the navigation equation (1). Taking into account (10) and the considerations carried out in [2, 4], the probability density function $p(\boldsymbol{\rho};\boldsymbol{\theta})$ in the two-dimensional space can be described by the equation

$$p(\boldsymbol{\rho};\boldsymbol{\theta}) = \frac{1}{(2\pi\sigma^2)^{\frac{N-1}{2}}}\exp\left\{-\frac{1}{2\sigma^2}\sum_{i=1}^{N-1}[\Delta d_i \right.$$
$$-\left(\sqrt{(X_{i+1}-x)^2+(Y_{i+1}-y)^2}\right.$$
$$\left.\left.-\sqrt{(X_i-x)^2+(Y_i-y)^2}+d_{rp}\right)\right]^2\right\} \tag{11}$$

where $\boldsymbol{\rho}$ is a vector whose elements represent virtual distance differences Δd_i, $\boldsymbol{\theta}$ is a vector of estimated coordinates (x, y), and σ is the standard deviation of virtual measurements of

distance differences. The Fisher information matrix takes the form

$$\mathbf{I}(\boldsymbol{\theta}) = \begin{bmatrix} -E\left[\dfrac{\partial^2 \ln p(\boldsymbol{\rho};\boldsymbol{\theta})}{\partial x^2}\right] & -E\left[\dfrac{\partial^2 \ln p(\boldsymbol{\rho};\boldsymbol{\theta})}{\partial x \partial y}\right] \\ -E\left[\dfrac{\partial^2 \ln p(\boldsymbol{\rho};\boldsymbol{\theta})}{\partial y \partial x}\right] & -E\left[\dfrac{\partial^2 \ln p(\boldsymbol{\rho};\boldsymbol{\theta})}{\partial y^2}\right] \end{bmatrix} \tag{12}$$

where (see Appendix B)

$$\frac{\partial^2 \ln p(\boldsymbol{\rho};\boldsymbol{\theta})}{\partial x^2} = -\frac{1}{\sigma^2}\sum_{i=1}^{N-1}\left[\frac{(X_{i+1}-x)}{\sqrt{(X_{i+1}-x)^2+(Y_{i+1}-y)^2}}\right.$$
$$\left.-\frac{(X_i-x)}{\sqrt{(X_i-x)^2+(Y_i-y)^2}}\right]^2 \tag{13}$$

$$\frac{\partial^2 \ln p(\boldsymbol{\rho};\boldsymbol{\theta})}{\partial x \partial y} = -\frac{1}{\sigma^2}\sum_{i=1}^{N-1}\left[\frac{(X_{i+1}-x)}{\sqrt{(X_{i+1}-x)^2+(Y_{i+1}-y)^2}}\right.$$
$$\left.-\frac{(X_i-x)}{\sqrt{(X_i-x)^2+(Y_i-y)^2}}\right]$$
$$\cdot\left[\frac{(Y_{i+1}-y)}{\sqrt{(X_{i+1}-x)^2+(Y_{i+1}-y)^2}}\right.$$
$$\left.-\frac{(Y_i-y)}{\sqrt{(X_i-x)^2+(Y_i-y)^2}}\right] \tag{14}$$

$$\frac{\partial^2 \ln p(\boldsymbol{\rho};\boldsymbol{\theta})}{\partial y \partial x} = -\frac{1}{\sigma^2}\sum_{i=1}^{N-1}\left[\frac{(Y_{i+1}-y)}{\sqrt{(X_{i+1}-x)^2+(Y_{i+1}-y)^2}}\right.$$
$$\left.-\frac{(Y_i-y)}{\sqrt{(X_i-x)^2+(Y_i-y)^2}}\right]$$
$$\cdot\left[\frac{(X_{i+1}-x)}{\sqrt{(X_{i+1}-x)^2+(Y_{i+1}-y)^2}}\right.$$
$$\left.-\frac{(X_i-x)}{\sqrt{(X_i-x)^2+(Y_i-y)^2}}\right] \tag{15}$$

$$\frac{\partial^2 \ln p(\boldsymbol{\rho};\boldsymbol{\theta})}{\partial y^2} = -\frac{1}{\sigma^2}\sum_{i=1}^{N-1}\left[\frac{(Y_{i+1}-y)}{\sqrt{(X_{i+1}-x)^2+(Y_{i+1}-y)^2}}\right.$$
$$\left.-\frac{(Y_i-y)}{\sqrt{(X_i-x)^2+(Y_i-y)^2}}\right]^2 \tag{16}$$

The above relationships were used to carry out numerical calculations and simulation tests. The results are presented in the next section.

VI. SIMULATION RESULTS

The results of numerical calculations and simulation studies for the proposed method are presented on the basis of the adopted sensor network model. This research is focused on the following areas:

- Analysis of the PDoP coefficient,
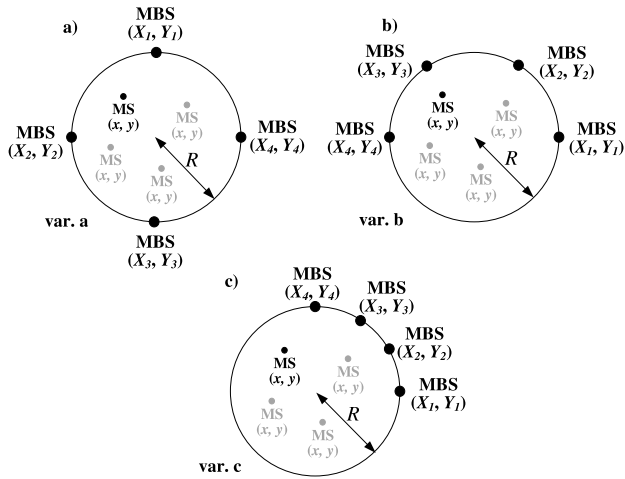- CRLB for the proposed method,
- Effectiveness of the method.

FIGURE 5. Applied topologies of sensor networks for simulation studies.

FIGURE 6. Correlation coefficient as a function of the number of random values generated.

FIGURE 7. The CDFs of the PDoP for the proposed method.

A. SIMULATION MODEL

The quality of position estimation in the developed radiolocation method was evaluated on the basis of the results of simulation tests. During the simulation analyses, three variants (a, b and c) were considered, which faithfully represent the real working conditions of the system:

a) MBS moved around a full circle with an R-radius, inside of which the measuring sensor was randomly placed (var. a),

b) MBS moved around a 1/2 circle, while the location of MS was the same as before (var. b),

c) MBS moved around a 1/4 circle, and MS was positioned similar to the previous ones (var. c),

as shown in Fig. 5.

The simulation tool was developed in the universal mathematical computational environment, MATLAB. During the simulation tests, the error of measurement of virtual distance difference with normal distribution (δ_d) was taken into account. To model this error, the *randn* function was used in the following way

$$\delta_d = \sigma \cdot randn \qquad (17)$$

where σ is the standard deviation of the virtual distance difference measurements. Before testing, the degree of correlation between the sequence of random numbers generated by the *randn* function and the Gaussian distribution describing the given random variable (a key parameter in modelling phenomena occurring in radiolocation systems) was checked in the MATLAB environment. For different sample sizes, correlation coefficients of probability distribution for generated sequences of random numbers with the Gaussian distribution were determined. The obtained results are presented in Fig. 6.

This figure shows, among other things, that in order to estimate a single statistic, the course of the simulation should be repeated many times. Therefore, in the conducted simulation studies, it was assumed that each case will be repeated 10,000 times (for this value, the correlation coefficient from
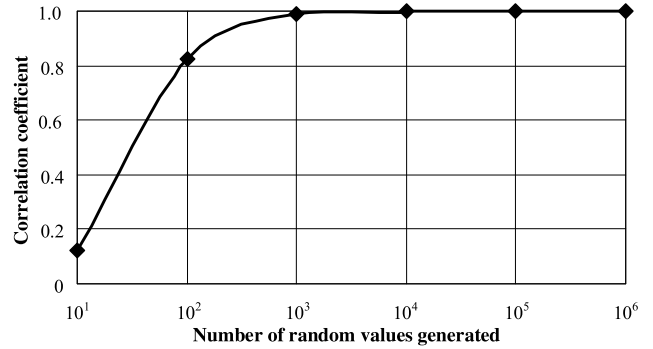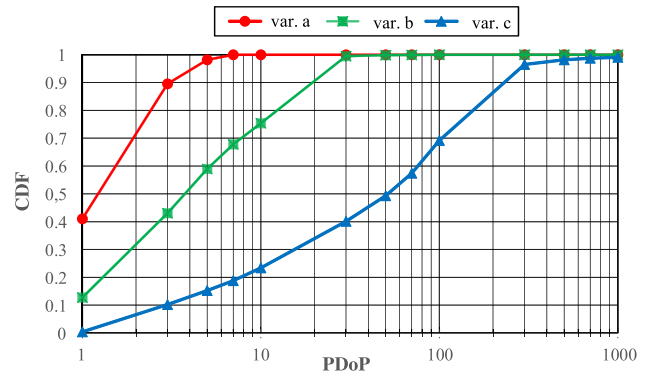
Fig. 6 is close to unity). Increasing the number of repetitions above this value does not practically improve the reliability of the obtained results, but only increases the duration of the simulation studies.

B. ANALYSIS OF PDOP COEFFICIENT

First, the analysis of the PDoP coefficient for the three topologies of the sensor network discussed above was carried out. Using (7), numerical calculations were performed in order to determine the cumulative distribution function (CDF) of the PDoP coefficient for the proposed radiolocation method [28]. The obtained characteristics (Fig. 7) show that the value of this coefficient in 100 % of the cases does not exceed the value of 10 for the configuration of a sensor network in which a MBS moves around the whole circle. Therefore, it can be expected that the resultant error of the MS's position estimation will be small, and it is the most advantageous variant of the network configuration. On the other hand, the least favorable configuration of the sensor network occurs in the third variant, in which the MBS moves around only 1/4 of the circle. The value of the PDoP coefficient not exceeding 10 occurs in only 25 % of the analyzed cases. Intermediate results were obtained for the configuration of the sensor network in which the MBS moved in 1/2 circle — a value of not higher than 10 for the PDoP coefficient was obtained for 75 % of the analyzed cases.
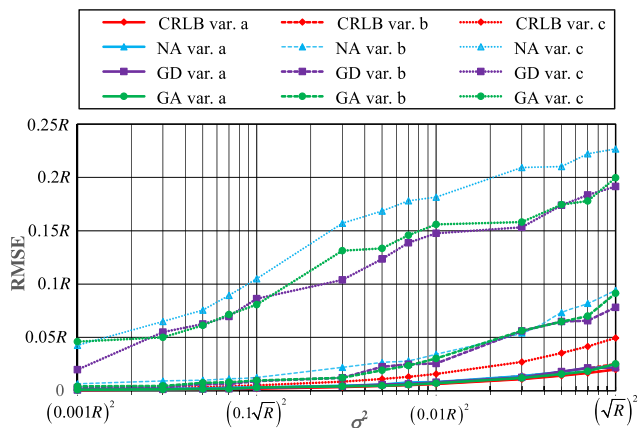
FIGURE 8. RMSE of MS position estimation as a function of the variance of virtual distance difference measurement errors σ^2 for Newton's algorithm (NA), gradient descent algorithm (GD), genetic algorithm (GA), and CRLB for three variants of sensor network configuration.

To sum up, it can be concluded that the value of the PDoP coefficient for the considered method in the variants of the configuration of the sensor network that were accepted for research change from less than one to several dozen, while there are such areas for which the value of this coefficient rapidly increases, striving for several hundred and more. This means that in these areas, problems of reversal of the matrix described in (7) and relatively large values of errors of MS position estimation can be expected.

C. CRLB FOR THE PROPOSED METHOD

Using (11) through (16), numerical calculations and simulation studies were carried out in order to determine the average root mean squared error in the function of variance of errors in virtual distance difference measurements between the measuring sensor and the mobile base station. The RMSE error of the localized object was determined on the basis of Cramér-Rao lower bound analysis, as well as calculated using Newton's algorithm, the gradient descent algorithm, and a genetic algorithm. These errors and the variance of virtual distance measurement errors were related to dimension R in the adopted model of simulation environment, which is described in Section VIA. The results presented in Fig. 8 were obtained for 10,000 random positions of the object in the examined area. In the NA and GA algorithms, the same maximum number of iterations equal to 1,000, and the number of potential solutions in the genetic algorithm ($w = 1\,024$) — the size of the matrix of solutions — were also adopted. For the gradient descent algorithm, the number of iterations was increased to 10^5. Moreover, the calculations took into account the three variants of the sensor network configuration. The individual axes of the graphs in Fig. 8 are purposely scaled to the size of the research area — to the R-radius of the research area. This approach enables easy scaling of the obtained results to the size of various areas where the accuracy of the virtual distance difference measurements is a given percentage of its radius. For example, for a circle-shaped

area with a radius of $R = 1000$ m, the variance $(0.01R)^2$ represents 100 m^2, i.e. the standard deviation of errors in the measurement of virtual distance differences represents 1 % of the radius.

The results obtained in Fig. 8 are as expected. The CRLB, depending on the assumed variance of the errors of the virtual distance difference measurements, oscillates between $0.001R$ and $0.05R$. This means that for the example considered above, the accuracy of the radiolocation method is limited to a range from 1 m to 50 m in a circular area with a radius of 1 km (Fig. 8). In light of this, the accuracy obtained with all algorithms under consideration is several times worse than the CRLB depending on the configuration variants of the sensor network.

As we know, the NA and GD iterative algorithms are sensitive to the initial solution vector, which should be close to the right solution. In the simulation studies, the initial value of this vector was always set to the center of the circular area of operation. However, it is clear that the best results are obtained for variant a) of the sensor network configuration, for which the MBS moves evenly throughout the circle of the analyzed area. On the other hand, the implemented genetic algorithm does not guarantee the convergence to the global extremum [9]. Qualitatively obtained GA results are located between the results obtained with the NA and GD.

D. EFFECTIVENESS OF THE METHOD

Next, a comparative analysis of MS position estimation accuracy was carried out in the proposed in Fig. 5 variants of sensor network configuration using three algorithms: Newton, gradient descent, and genetic for selected values of errors in measurements of virtual distance differences between the MBS and MS.

At this point, it should be stressed that the choice of the above three algorithms to solve the system of non-linear equations was only dictated by the desire to show that such a solution exists and can be found using iterative algorithms even if the closed form solution is not known. The aim of the paper was therefore to present a new locating method, not to discuss or optimize the algorithms used in the proposed solution.

On the basis of the results obtained from the simulation studies, the CDF of the absolute error δ, described in (18), for the three considered variants of the topology of a sensor network were plotted.

$$\delta = \sqrt{\left(\hat{x} - x\right)^2 + \left(\hat{y} - y\right)^2} \qquad (18)$$

where $(\hat{x}, \hat{y})$ are MS coordinate estimates. For each topology, the accuracy of MS position estimation was analyzed using three algorithms and two values of standard deviations σ of the virtual distance differences measurement errors. For the purpose of generalization of conclusions, the results obtained were expressed in the R-radius length of the studied area. The results of the simulation tests are presented in Fig. 9 through Fig. 12, while two basic cases are considered. The first case
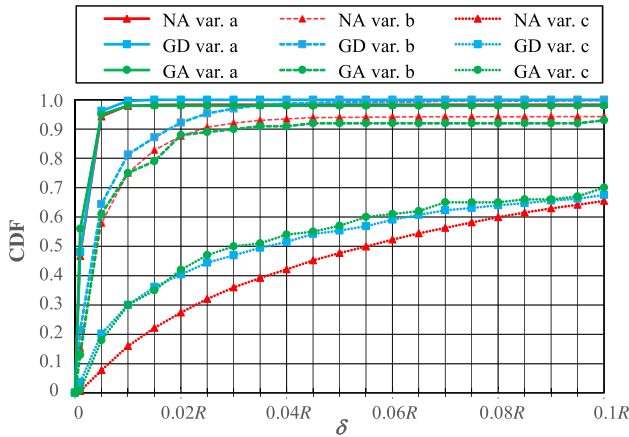
FIGURE 9. The CDFs of the absolute position error δ for the proposed method for three sensor network configuration variants using the Newton (NA), gradient descent (GD), and genetic (GA) algorithms. It was also assumed that the MBS coordinates were flawless and the error in measuring virtual distance differences were affected by $\sigma = 0.001R$.
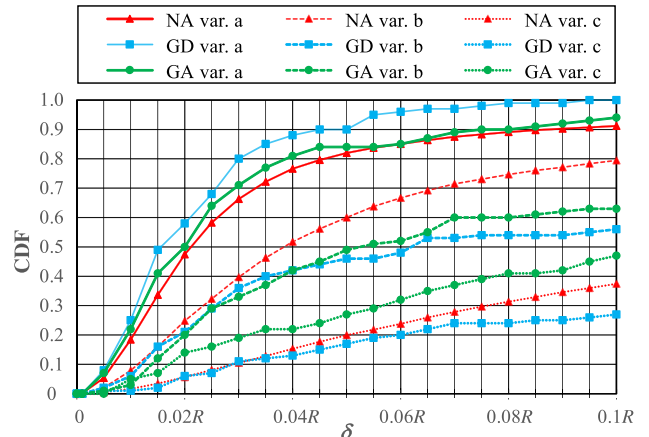

FIGURE 11. The CDFs of the absolute position error δ for the proposed method for three sensor network configuration variants using the Newton (NA), gradient descent (GD), and genetic (GA) algorithms. It was also assumed that the error in measuring virtual distance differences and the coordinates of the MBS were affected by $\sigma = 0.001R$ and $0.01R$, respectively.
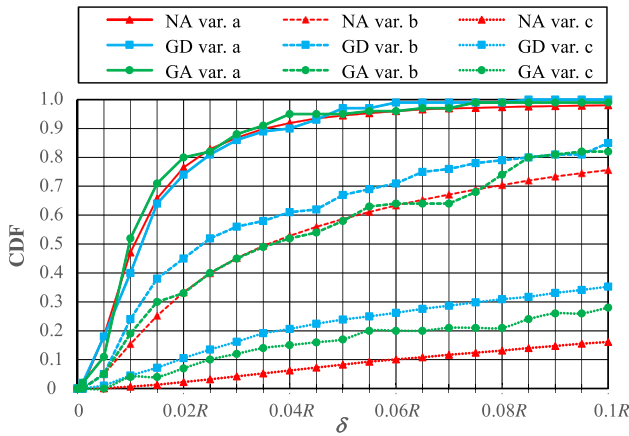

FIGURE 10. The CDFs of the absolute position error δ for the proposed method for three sensor network configuration variants using the Newton (NA), gradient descent (GD), and genetic (GA) algorithms. It was also assumed that MBS coordinates were flawless and the error in measuring virtual distance differences were affected by $\sigma = 0.01R$.
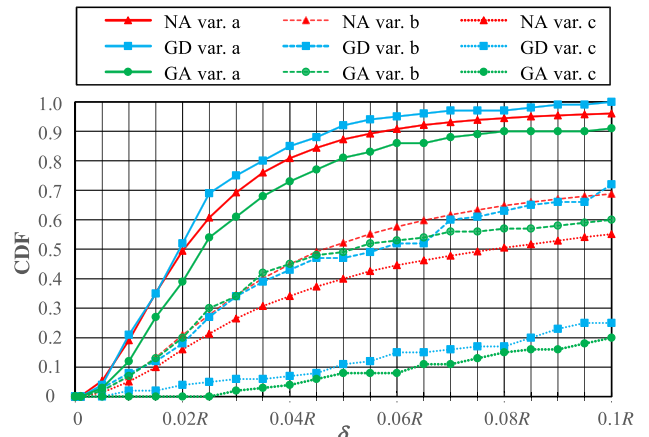

FIGURE 12. The CDFs of the absolute position error δ for the proposed method for three sensor network configuration variants using the Newton (NA), gradient descent (GD), and genetic (GA) algorithms. It was also assumed that the error in measuring virtual distance differences and the coordinates of the MBS were affected by $\sigma = 0.01R$.

concerned the assumption that in the MS position estimation process, the mobile base station was characterized by flawless coordinates, while in the second one, the coordinates of the MBS were burdened with $\sigma = 0.01R$ error. Two values of virtual distance difference errors between the MBS and MS equal to $0.001R$ (Fig. 9 and Fig. 11) and $0.01R$ (Fig. 10 and Fig. 12) were also considered. As expected, the best results were achieved for variant a, and the worst for variant c. Analyzing the results presented in Fig. 9, it can be concluded that the CDF for individual variants of sensor network configuration are grouped in two significantly different areas.

The first area, in which a significant increase in the value of the CDF can be observed along with an increase in the absolute error, is reserved for relatively small values of standard deviations σ for measurement of virtual distance differences between the MBS and MS and for variant a and variant b of the network configuration. The shape of the curves in this area

are typical for Gaussian error distribution and zero average values. In the second area for variant c, the increase in the value of the CDF is mild as the absolute error increases. From the analysis of the CDF graphs, it can also be concluded that, in general, the gradient descent algorithm provides more accurate estimation of the MS position compared to the other algorithms: Newton and genetic.

In the other three diagrams (Fig. 10 through Fig. 12), the CDF curves as a function of absolute error are arranged in three distinct groups. Each of these groups is assigned to a proposed variant of the MBS's trajectory. In a favorable sensor network configuration (variant a), the best results were achieved using the gradient descent algorithm, regardless of the assumed error of measurement of virtual distance differences between the MBS and MS as well as the assumed error of determining the MBS's coordinates. For the other two
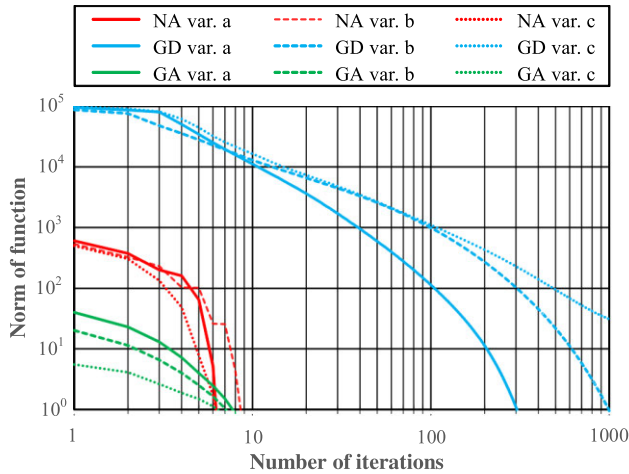
FIGURE 13. Norm of navigation equation as a function of the number of iterations for three sensor network configuration variants using the Newton (NA), gradient descent (GD) and genetic (GA) algorithms. It was also assumed that the error in measuring virtual distance differences and the coordinates of the MBS were affected by $\sigma = 0.001R$ and $0.01R$, respectively.

variants of the network configuration, b and c, satisfactory results were obtained for the genetic and Newton algorithms.

For large values of measurement errors of virtual distance differences (10 % of the radius of the area where the sensor network is located) and for the proposed network configuration in variant c, the results obtained are below expectations.

At the end of this section, it is also worth considering the convergence of the algorithms used to solve the system of non-linear equations. In Fig. 13, we plot the changes in the norm of the criterion function as a function of the number of iterations. The form of the criterion function depends on the algorithm under consideration (see Appendix A). For the NA, the norm of a criterion function is described as $||(\mathbf{J}^T \cdot \mathbf{J})^{-1} \cdot \mathbf{J}^T \cdot \mathbf{f}||$, for the GD algorithm, the norm is $||0.5 \cdot \mathbf{f}^T \cdot \mathbf{f}||$, while for the GA, the norm is $||\mathbf{f}||$, with the vector $\mathbf{f}$ being described by (3) and matrix $\mathbf{J}$ described by (5). The algorithm convergence studies were performed for a case where it was assumed that the error in measuring virtual distance differences and the coordinates of the MBS were modeled by $\sigma = 0.001R$ and $0.01R$, respectively.

As was to be expected, the fastest converging algorithms among those considered were NA and GA. The value of the criterion function equal to or less than one is obtained after several iterations, but in the case of the NA, it results from the properties of this algorithm, while for the GA, it results from the size of the table of potential solutions, which in the considered case was $w = 1024$. The least preferred in this respect was the GD algorithm. At least several hundred iterations were needed to obtain the value of the criterion function at the unity level and below. However, in the era of dynamic performance developments of computational systems, the solution of the system of non-linear equations with any of the proposed algorithms leads to the realization of this process practically in real-time.

It is also worth noting that the convergence of the GA is not guaranteed, hence its final results may be characterized by higher final errors despite more iterations than the other algorithms. In addition, it is an algorithm based on random searches of different parts of the solution space. This provides the opportunity to find a global solution, but it does not guarantee it. The other two algorithms (NA and GD) use information about the variability of the target function around the current search point, hence should find a minimum of target functions faster and give a more accurate solution, but in a case where the target function has not only a global minimum but also some local minima, the convergence of NA and GD to the global minimum is again not guaranteed.

The analysis of the results obtained for the proposed locating method leads to the following conclusions:

- regardless of the measurement error values of virtual distance differences, the best results were obtained for the gradient descent algorithm,
- for the variant a sensor network configuration, the error values are on average 15 % higher for the NA and GA algorithms compared to the gradient descent algorithm,
- for variants b and c of the sensor network configuration, the MS position estimation errors are on average between a few and a dozen percent higher for the NA and GA algorithms compared to the GD algorithm,
- in practical applications of the proposed locating method, it is recommended that variant a or b of the sensor network configuration be used,
- the use of any algorithm (NA, GD or GA) to solve a system of non-linear equations allows the implementation of the MS position estimation practically in real-time.

VII. CONCLUSION
The paper presents an innovative asynchronous radiolocation method for application in the IoT. A novelty in this method is to perform measurements of virtual distance differences between a mobile base station and a stationary measuring sensor. A mathematical analysis of the proposed method was carried out taking into account the implementation details of the Newton, gradient descent, and genetic algorithms to solve the system of positional equations.

Next, attention was paid to the unfavorable value of the PDoP coefficient, assuming that it is determined in an analogous way to the classical solutions of radiolocation systems, i.e. on the basis of Jacobian matrix knowledge. For obvious reasons, in the studied area, there are places particularly privileged in terms of this coefficient.

In the next section of this paper, the Cramér-Rao lower bound, i.e. the limit of accuracy of this method, which is a reference point for the evaluation of the developed algorithms of the estimation of the object's position, with the assumption of a Gaussian distribution of measurement errors, was presented. The set of curves representing the root mean square error of the estimation of the object's position as a function of absolute error δ were plotted. The results obtained with the

---

Algorithm 1 Pseudocode of Newton's Algorithm

$k \leftarrow 1$ ▷ Iteration counter
$x \leftarrow 0$ ▷ Inital coordinates of MS
$y \leftarrow 0$
while $k < n_{iter}$ **and** $norm > t_{\text{hold}}$ **do**
     $d_1 \leftarrow \sqrt{(X_1 - x)^2 + (Y_1 - y)^2}$ ▷ Estimated distances
                   between MS and MBS
     $d_2 \leftarrow \sqrt{(X_2 - x)^2 + (Y_2 - y)^2}$
     $d_3 \leftarrow \sqrt{(X_3 - x)^2 + (Y_3 - y)^2}$
     $d_4 \leftarrow \sqrt{(X_4 - x)^2 + (Y_4 - y)^2}$
     $\mathbf{J}_{1,1} \leftarrow \frac{X_1 - x}{d_1} + \frac{2 \cdot (x - X_2)}{d_2} + \frac{X_3 - x}{d_3}$ ▷ Jacobian
     $\mathbf{J}_{2,1} \leftarrow \frac{X_1 - x}{d_1} + \frac{x - X_2}{d_2} + \frac{x - X_3}{d_3} + \frac{X_4 - x}{d_4}$
     $\mathbf{J}_{1,2} + \frac{Y_1 - y}{d_1} + \frac{2 \cdot (y - Y_2)}{d_2} + \frac{Y_3 - y}{d_3}$
     $\mathbf{J}_{2,2} + \frac{Y_1 - y}{d_1} + \frac{y - Y_2}{d_2} + \frac{y - y_3}{d_3} + \frac{Y_4 - y}{d_4}$
     $\mathbf{f}_{1,1} \leftarrow \Delta d_2 - \Delta d_1 - d_3 + 2 \cdot d_2 - d_1$ ▷ Vector f
     $\mathbf{f}_{2,1} \leftarrow \Delta d_3 - \Delta d_1 - d_4 + d_3 + d_2 - d_1$
     $\mathbf{h} \leftarrow -\left(\mathbf{J^T} \cdot \mathbf{J}\right)^{-1} \cdot \mathbf{J^T} \cdot \mathbf{f}$ ▷   Correction of MS
                         coordinates
     $x \leftarrow x + \mathbf{h}_1$
     $y \leftarrow y + \mathbf{h}_2$
     $norm \leftarrow \|\mathbf{h}\|$ ▷ h vector norm
     $k \leftarrow k + 1$ ▷ Iteration counter
end while

Algorithm 2 Pseudocode of the Gradient Descent Algorithm

Require: $\lambda > 0$ ▷ Initial correction rate coefficient
   $k \leftarrow 1$ ▷ Iteration counter
   $x \leftarrow 0$ ▷ Inital coordinates of MS
   $y \leftarrow 0$
   while $k < n_{iter}$ **and** $norm > t_{hold}$ **do**
     $d_1 \leftarrow \sqrt{(X_1 - x)^2 + (Y_1 - y)^2}$ ▷ Etimated distances
                   between MS and MBS
     $d_2 \leftarrow \sqrt{(X_2 - x)^2 + (Y_2 - y)^2}$
     $d_3 \leftarrow \sqrt{(X_3 - x)^2 + (Y_3 - y)^2}$
     $d_4 \leftarrow \sqrt{(X_4 - x)^2 + (Y_4 - y)^2}$
     $\mathbf{J}_{1,1} \leftarrow \frac{X_1 - x}{d_1} + \frac{2 \cdot (x - X_2)}{d_2} + \frac{X_3 - x}{d_3}$ ▷ Jacobian
     $\mathbf{J}_{2,1} \leftarrow \frac{X_1 - x}{d_1} + \frac{x - X_2}{d_2} + \frac{x - X_3}{d_3} + \frac{X_4 - x}{d_4}$
     $\mathbf{J}_{1,2} \leftarrow \frac{Y_1 - y}{d_1} + \frac{2 \cdot (y - Y_2)}{d_2} + \frac{Y_3 - y}{d_3}$
     $\mathbf{J}_{2,2} \leftarrow \frac{Y_1 - y}{d_1} + \frac{y - Y_2}{d_2} + \frac{y - Y_3}{d_3} + \frac{Y_4 - y}{d_4}$
     $\mathbf{f}_{1,1} \leftarrow \Delta d_2 - \Delta d_1 - d_3 + 2 \cdot d_2 - d_1$ ▷ Vector f
     $\mathbf{f}_{2,1} \leftarrow \Delta d_3 - \Delta d_1 - d_4 + d_3 + d_2 - d_1$
     $norm_k \leftarrow 0.5 \cdot \mathbf{f^T} \cdot \mathbf{f}$ ▷ f vector norm
     if $norm_k > norm_{k-1}$ **then**
         $\lambda \leftarrow \lambda / 2$ ▷ Reduction in case of divergence
     end if
     $\mathbf{h} \leftarrow -\lambda \cdot \mathbf{J^T} \cdot \mathbf{f}$ ▷ Correction of MS coordinates
     $x \leftarrow x + \mathbf{h}_1$
     $y \leftarrow y + \mathbf{h}_2$
     $k \leftarrow k + 1$ ▷ Iteration counter
end while

---

use of gradient descent algorithm are the closest to the CRLB boundary.

The results of complex simulation studies of the proposed asynchronous method for four cases and for various system parameters were presented. In total, four sets of characteristics of the CDF as a function of absolute error were plotted. The estimation of the MS position was performed with the use of the three abovementioned algorithms: Newton, gradient descent, and genetic. The analysis shows that the most accurate results for all variants of sensor network configuration can be obtained using the gradient descent algorithm. Slightly worse results were obtained for the genetic algorithm. The worst result was obtained for Newton's algorithm, especially for relatively large assumed measurement errors.

The proposed method can be widely used in IoT applications, especially where local sensor networks (e.g. related to measurements or surveillance of a designated area) are outside of the cellular network coverage area. In local sensor networks, assuming low-cost operation, where the equipment of the measurement sensors has been reduced to a minimum, there is a need for their location. According to the analyses and simulation tests, the accuracy of the method in different configurations of a sensor network can satisfy many applications. However, a certain limitation of the method may be the time between measurements. The accuracy of the measurements depends on the stability of the frequency standard placed on the drone. For example, if the stability of the frequency standard is 10^{-9}, taking measurements at 10 second intervals leads to an error of distance measurements of 3 m.

APPENDIXES
APPENDIX A
See Algorithms 1 and 2.

APPENDIX B
The second derivatives of Fisher's information matrix in (13) to (16) are presented without components that are equal to zero when the coordinates of the mobile nodes match the results of the virtual distance measurements. Full expressions for these derivatives are presented below. First, let's focus on the relationship describing the first and second derivative $p(\boldsymbol{\rho}; \boldsymbol{\theta})$ to the x variable:

$$\frac{\partial \ln p(\boldsymbol{\rho}; \boldsymbol{\theta})}{\partial x}$$

$$= -\frac{1}{\sigma^2} \sum_{i=1}^{N-1} \left\{ \left[-\sqrt{(X_{i+1} - x)^2 + (Y_{i+1} - y)^2} \right. \right.$$

$$+ \sqrt{(X_i - x)^2 + (Y_i - y)^2} - d_{rp} + \Delta d_i \bigg]$$

$$\left. \cdot \left[\frac{(X_{i+1} - x)}{\sqrt{(X_{i+1} - x)^2 + (Y_{i+1} - y)^2}} - \frac{(X_i - x)}{\sqrt{(X_i - x)^2 + (Y_i - y)^2}} \right] \right\}$$

$$\tag{B1}$$

$$\frac{\partial^2 \ln p(\boldsymbol{\rho}; \boldsymbol{\theta})}{\partial x^2}$$

$$= -\frac{1}{\sigma^2} \sum_{i=1}^{N-1} \left\{ \left[-\sqrt{(X_{i+1}-x)^2 + (Y_{i+1}-y)^2} \right.\right.$$

$$+ \left. \sqrt{(X_i-x)^2 + (Y_i-y)^2} - d_{rp} + \Delta d_i \right]$$

$$\cdot \left[\frac{(X_{i+1}-x)^2}{\left[(X_{i+1}-x)^2 + (Y_{i+1}-y)^2\right]^{\frac{3}{2}}} - \frac{(X_i-x)^2}{\left[(X_i-x)^2 + (Y_i-y)^2\right]^{\frac{3}{2}}} \right.$$

$$\left. - \frac{1}{\sqrt{(X_{i+1}-x)^2 + (Y_{i+1}-y)^2}} + \frac{1}{\sqrt{(X_i-x)^2 + (Y_i-y)^2}} \right]$$

$$\left. + \left[\frac{(X_{i+1}-x)}{\sqrt{(X_{i+1}-x)^2 + (Y_{i+1}-y)^2}} - \frac{(X_i-x)}{\sqrt{(X_i-x)^2 + (Y_i-y)^2}} \right]^2 \right\}$$

$$\tag{B2}$$

Taking into account expression (B1), it can be seen that the first square bracket of the second derivative $p(\boldsymbol{\rho}; \boldsymbol{\theta})$ function equals zero, so that ultimately the second derivative of this function takes the form of (13).

Now let's look at the form of the second derivative of the $p(\boldsymbol{\rho}; \boldsymbol{\theta})$ function relative to the x and y variables.

$$\frac{\partial^2 \ln p(\boldsymbol{\rho}; \boldsymbol{\theta})}{\partial x \partial y}$$

$$= -\frac{1}{\sigma^2} \sum_{i=1}^{N-1} \left\{ \left[-\sqrt{(X_{i+1}-x)^2 + (Y_{i+1}-y)^2} \right.\right.$$

$$+ \left. \sqrt{(X_i-x)^2 + (Y_i-y)^2} - d_{rp} + \Delta d_i \right]$$

$$\cdot \left[\frac{(X_{i+1}-x) \cdot (Y_{i+1}-y)}{\left[(X_{i+1}-x)^2 + (Y_{i+1}-y)^2\right]^{\frac{3}{2}}} - \frac{(X_i-x) \cdot (Y_i-y)}{\left[(X_i-x)^2 + (Y_i-y)^2\right]^{\frac{3}{2}}} \right]$$

$$+ \left[\frac{(X_{i+1}-x)}{\sqrt{(X_{i+1}-x)^2 + (Y_{i+1}-y)^2}} - \frac{(X_i-x)}{\sqrt{(X_i-x)^2 + (Y_i-y)^2}} \right]$$

$$\left. \cdot \left[\frac{(Y_{i+1}-y)}{\sqrt{(X_{i+1}-x)^2 + (Y_{i+1}-y)^2}} - \frac{(Y_i-y)}{\sqrt{(X_i-x)^2 + (Y_i-y)^2}} \right] \right\}$$

$$\tag{B3}$$

As before, the first square bracket of the second derivative $p(\boldsymbol{\rho}; \boldsymbol{\theta})$ function equals zero, so that ultimately the second derivative of this function takes the form of (14). In the same way, relationships (15) and (16) can be derived.

REFERENCES

[1] J. D. Bard and F. M. Ham, "Time difference of arrival dilution of precision and applications," *IEEE Trans. Signal Process.*, vol. 47, no. 2, pp. 521–523, Feb. 1999, doi: 10.1109/78.740135.

[2] C. Chang and A. Sahai, "Cramér-Rao-type bounds for localization," *EURASIP J. Adv. Signal Process.*, vol. 2006, Dec. 2006, Art. no. 094287, doi: 10.1155/ASP/2006/94287.

[3] Z. Chen, F. Xia, T. Huang, F. Bu, and H. Wang, "A localization method for the Internet of Things," *J. Supercomput.*, vol. 63, no. 3, pp. 657–674, Mar. 2013, doi: 10.1007/s11227-011-0693-2.

[4] *Universal Mobile Telecommunications System (UMTS); Evaluation of the Inclusion of Path Loss Based Location Technology in the UTRAN, ETSI TR 125 907 ver. 9.0.1*, Eur. Telecommun. Standards Inst., Sophia Antipolis, France, Feb. 2010.

[5] D. E. Fasshauer, *Meshfree Approximation Methods with MATLAB*. Singapore: World Scientific Publishing, 2007.

[6] J. Figueiras and S. Frattasi, *Mobile Positioning and Tracking: From Conventional to Cooperative Techniques*. London, U.K.: Wiley, 2010.

[7] R. Fletcher and M. J. D. Powell, "A rapidly convergent descent method for minimization," *Comput. J.*, vol. 6, no. 2, pp. 163–168, Aug. 1963, doi: 10.1093/comjnl/6.2.163.

[8] W. Foy, "Position-location solutions by Taylor-series estimation," *IEEE Trans. Aerosp. Electron. Syst.*, vols. AES–12, no. 2, pp. 187–194, Mar. 1976, doi: 10.1109/TAES.1976.308294.

[9] R. F. Hartl, "A global convergence proof for a class of genetic algorithms," Inst. Manage., Univ. Vienna, Tech. Rep., Vienna, Austria, Jan. 1990, pp. 1–6. [Online]. Available: http://citeseerx.ist.psu.edu/viewdoc/summary?doi=10.1.1.330.1662

[10] C. L. Karr, B. Weck, and L. M. Freeman, "Solutions to systems of nonlinear equations via a genetic algorithm," *Eng. Appl. Artif. Intell.*, vol. 11, no. 3, pp. 369–375, Jun. 1998, doi: 10.1016/S0952-1976(97)00067-5.

[11] S. M. Kay, *Fundamentals of Statistical Signal Processing: Estimation Theory*. Upper Saddle River, NJ, USA: Prentice-Hall, 1993.

[12] P. Lea, *Internet of Things for Architects*. Birmingham, U.K.: Packt Publishing, 2018.

[13] X. Lin, J. Bergman, F. Gunnarsson, O. Liberg, S. M. Razavi, H. S. Razaghi, H. Rydn, and Y. Sui, "Positioning for the Internet of Things: A 3GPP perspective," *IEEE Commun. Mag.*, vol. 55, no. 12, pp. 179–185, Dec. 2017, doi: 10.1109/MCOM.2017.1700269.

[14] Y. Liu and Z. Yang, *Localizability: Location-awareness Technology for Wireless Networks*. New York, NY, USA: Springer, 2011.

[15] R. N. McDonough and A. D. Whalen, *Detection of Signals in Noise*, 2nd ed. San Diego, CA, USA: Academic, 1995.

[16] M. Miszewski, J. Sadowski, and J. Stefanski, "A method of transmitting information for the Internet of Things (IoT), especially outside the area of radio communications networks," Patent Appl. 432 108, Dec. 6, 2019.

[17] I. Nevat, G. W. Peters, K. Avnit, F. Septier, and L. Clavier, "Location of things: Geospatial tagging for IoT using Time-of-Arrival," *IEEE Trans. Signal Inf. Process. over Netw.*, vol. 2, no. 2, pp. 174–185, Jun. 2016, doi: 10.1109/TSIPN.2016.2531422.

[18] K. Radnosrati, G. Hendeby, C. Fritsche, F. Gunnarsson, and F. Gustafsson, "Performance of OTDOA positioning in narrowband IoT systems," in *Proc. IEEE 28th Annu. Int. Symp. Pers., Indoor, Mobile Radio Commun. (PIMRC)*, Oct. 2017, pp. 1–7, doi: 10.1109/PIMRC.2017.8292365.

[19] J. Sadowski and J. Stefanski, "Asynchronous phase-location system," *J. Mar. Eng. Technol.*, vol. 16, no. 4, pp. 400–408, Feb. 2017, doi: 10.1080/20464177.2017.1376372.

[20] J. Sadowski and J. Stefanski, "Asynchronous WAM with irregular pulse repetition," *J. Navigat.*, vol. 72, no. 1, pp. 85–100, Jan. 2019, doi: 10.1017/S0373463318000607.

[21] D.-H. Shin and T.-K. Sung, "Comparisons of error characteristics between TOA and TDOA positioning," *IEEE Trans. Aerosp. Electron. Syst.*, vol. 38, no. 1, pp. 307–311, Jan. 2002, doi: 10.1109/7.993253.

[22] R. C. Shit, S. Sharma, D. Puthal, and A. Y. Zomaya, "Location of things (LoT): A review and taxonomy of sensors localization in IoT infrastructure," *IEEE Commun. Surveys Tuts.*, vol. 20, no. 3, pp. 2028–2061, 3rd Quart., 2018, doi: 10.1109/COMST.2018.2798591.

[23] P. Silva, V. Kaseva, and E. Lohan, "Wireless positioning in IoT: A look at current and future trends," *Sensors*, vol. 18, no. 8, p. 2470, Jul. 2018, doi: 10.3390/s18082470.

[24] J. Stefanski, "Asynchronous time difference of arrival (ATDOA) method," *Pervas. Mobile Comput.*, vol. 23, pp. 80–88, Oct. 2015, doi: 10.1016/j.pmcj.2014.10.008.

[25] J. Stefanski and J. Sadowski, "TDOA versus ATDOA for wide area multilateration system," *EURASIP J. Wireless Commun. Netw.*, vol. 2018, no. 1, pp. 1–13, Dec. 2018, doi: 10.1186/s13638-018-1191-5.

[26] J. B. Y. Tsui, *Fundamentals of Global Positioning System Receivers: A Software Approach*. New York, NY, USA: Wiley, 2000.

[27] H. Yasuura, C. M. Kyung, Y. Liu, and Y. L. Lin, *Smart Sensors at the IoT Frontier*. Cham, Switzerland: Springer, 2017.

[28] R. Tiwari, S. Bhattacharya, P. K. Purohit, and A. K. Gwal, "Effect of TEC variation on GPS precise point at low latitude," *Open Atmos. Sci. J.*, vol. 3, no. 1, pp. 1–12, Jan. 2009, doi: 10.2174/1874282300903010001.

JACEK STEFANSKI (Member, IEEE) received the M.Sc., Ph.D., and D.Sc. degrees in telecommunications engineering from the Gdansk University of Technology (GUT), Poland, in 1993, 2000, and 2012, respectively.

From 1993 to 2000, he has worked as an Assistant Professor with the Department of Radio Communication Systems and Networks (DRCSN), GUT, where he has been working as an Associate Professor, since 2001. From 2005 to 2009, he has worked as an Assistant Professor with the National Institute of Telecommunications in the Gdansk Branch. He has been serving and as the Vice-Dean for organization of studies at the Faculty of Electronics, Telecommunications and Informatics, GUT, since 2016, and the Head of the DRCSN, since 2018. His research and development interests include analysis, simulation, design and measurement of cellular, wireless and trunked radio systems, techniques of digital modulation, channel coding, signal spreading, radio signal reception, measurement of radio wave propagation, field strength prediction, software radio design, location services, ad-hoc sensor networks, radio monitoring systems, and radio navigation systems. He is the author and a coauthor of more than 250 articles. He is also a coauthor of nine patents and over a dozen patent applications. He is a member of the Electromagnetic Compatibility Section of the Electronics and Telecommunications Committee of the Polish Academy of Sciences, and the Sub-Committee on Navigation, Communications and Search and Rescue in the International Maritime Organization. He is also a member of the Board of Associate Editors of the *International Journal of Electronics and Telecommunications*. He was awarded as a title of Professor by the President of Poland, in 2020.

JAROSLAW SADOWSKI received the M.Sc. degree in mobile radio communication systems from the Gdansk University of Technology, Gdansk, Poland, in 2002, the Ph.D. degree in radio communication, in 2010, and the D.Sc. degree in informatics and telecommunications, in 2019.

From 2002 to 2006, he was working in industry, designing and constructing 2G/3G base stations. Since 2007, he has been an Assistant Professor with the Department of Radio Communication Systems and Networks (DRCSN), Gdansk University of Technology. Since 2018, he has been the Deputy Head of the DRCSN. His research interests include localization in indoor environments, ultrawideband technology, and electromagnetic compatibility. He is a member of the Electromagnetic Compatibility Section of the Electronics and Telecommunications Committee of the Polish Academy of Sciences.

. . .